Self-organization of sepiolite fibbers in a biobased thermoset

Guillaume Falco, Françoise Giulieri, Nicolas Volle, Sophie Pagnotta, Nicolas Sbirrazzuoli, Edith Peuvrel-Disdier, Alice Mija

SELF-ORGANIZATION OF SEPIOLITE FIBBERS IN A BIOBASED THERMOSET

Guillaume Falco[1], Françoise Giulieri[2], Nicolas Volle[2], Sophie Pagnotta[3], Nicolas Sbirrazuoli[1], Edith Peuvrel-Disdier[4], Alice Mija[1]*

[1] Université Côte d'Azur, Université Nice-Sophia Antipolis, Institut de Chimie de Nice, UMR CNRS 7272, 06108 Nice Cedex 02, France

[2] *SAS PIGM'Azur* 4 Bd de CIMIEZ, Le Majestic 06000 Nice France

[3] Université Côte d'Azur, Université Nice-Sophia Antipolis, Centre Commun de Microscopie Appliquée, 06108 Nice Cedex 02, France

[4] MINES ParisTech, PSL Research University, CEMEF - Centre de Mise en Forme des Matériaux, UMR CNRS 7635, CS 10207, 06904 Sophia-Antipolis Cedex, France

*E-mail: Alice.Mija@unice.fr

Abstract:

Unusual self-organization of sepiolite fibbers have been found during the synthesis of sustainable nanocomposites. These auto-structured networks are synthesized starting with an epoxidized linseed oil (ELO), a bio-based hardener of dicarboxylic class and sepiolite fibbers. For the first time, the auto-organization of sepiolite fibbers into empty or solid spheres insight a bio-based thermoset matrix have been highlighted and synthesized. The influence of the thermoset formulation and the sepiolite concentration on self-organization are emphasized. The thermomechanical properties of nanocomposites have been investigated highlighting an increasing of elastic modulus from 30 to 40 % in the vitreous states and from 25 to 45 % in the rubbery state. This peculiar organization and behaviour of sepiolite, similar to that of surfactants, is of great interest as fundamental, applicative and industrial level.

Keywords: sustainable nanocomposites, bio-renewable resources, sepiolite, epoxidized vegetable oils, control of dispersion, self-organization

1. Introduction

Sustainable nanocomposites are a recent class of materials that are attracting a strong industrial and academic interest. This is largely due to the interest of bio-based resources but also to their good mechanical, thermal, electrical and optical properties [1] [2]. Commonly,

polymer nanocomposites are made by dispersing inorganic or organic nanoparticles into either thermoplastic or thermoset matrix [3] [4] [5] [6] [7] [8]. The high value of specific surface and the aspect ratio of nanoparticles enhance their interactions with the polymer, and permit to modulate the polymer performances [9] [10].

In epoxy thermosets chemistry and applications, vegetable oils have been proven theirs ability to produce materials with excellent thermomechanical properties [11] [12] [13]. Among all vegetable oils from sustainability purposes, our choice was focused on the linseed oil due to its high degree of functionalization [14] and its eco-friendly epoxidation process (enzymatic pathway) [15] [16]. To expand the carbon bio-based content on organic matrix, the epoxidized linseed oil (ELO) was reacted with a bio-based hardener of dicarboxylic class, named AcDiC, previously prepared [17] [18]. The choice of this association was motivated because of the excellent homogeneity and compatibility between ELO and the hardener combined with the non-toxicity of these both monomers.

Clays as additive for thermoplastic and thermosetting polymers have awakened considerable interest in the last decades, with the nano-composites [19] and bio-nanocomposites trend [20] [21] [22] [23] [24] [25]. Intercalated platelet clays are largely used and among them, montmorillonite and hectorite. The fibrous family clays like palygorskite or sepiolite were less employed in the development and applications of clay-based polymer nanocomposites. As far as sepiolite/polymer nanocomposites are concerned, only few studies have been reported in the literature. Nevertheless, the sepiolite was used to increase the mechanical properties as the tensile strength and stiffness of polymers as acrylates [26] [27], polyesters [28], epoxies [29] [30] [31], polyethylene [32], polypropylene [33] [34], polyamides [35] [36], polyurethanes [37], and biocompatible polymers [38] [39].

The sepiolite is a magnesium silicate included in the pseudo-phyllosilicate group. Structurally, sepiolite is formed by an alternation of blocks and cavities, forming tunnels and

channels (figure 1A), that grow up in the fibber direction. Two tetrahedral silica sheets sandwiching a central sheet of magnesium oxide-hydroxide compose each structural sepiolite block. The ideal half-unit cell formula of sepiolite is $[Mg_8Si_{12}O_{30}(OH)_4(OH_2)_4,8H_2O]$. The sepiolite fibber's surface is covered with silanol groups spaced at around 5 Å and located at the edges of the channels. The dimensions of the cross section of sepiolite tunnels are 3.7 Å x 10.6 Å [40] [41] [42].

The sepiolite is extracted from carrier rock and grinded (crushed) by micronization technique. Agglomerates sepiolite bundles constitute the obtained sepiolite powder. When this powder is dispersed in matrices, isolated state fibbers called "lath" are rare. Even after an effective dispersion, they are associated in parallel with each other in the form of "rods" that tend to be organized almost parallel to form bundles (figure 1B). The size of the unitary fibber (lath) is around 15 nm × 30 nm × 500-5000 nm.

The sepiolite has several peculiarities that make it a very original filler. Firstly, its fibrous state gives it, from very low concentrations, specific rheological [29] and hydrotropic behaviours, an ability to achieve percolation effects and therefore a strengthening [26] [29] [35] [43] [44] [45] and finally a tendency to associate in aqueous and non-aqueous media [46] [47]. Secondly, the presence of many surface silanol groups makes surface modifications easy and efficient to adapt the clay to many environments [27]. Finally, the existence of micro, meso- and macropores allows incorporation of organic molecules such as dyes, drugs, antifungals or other active molecules [27] [48] [49].

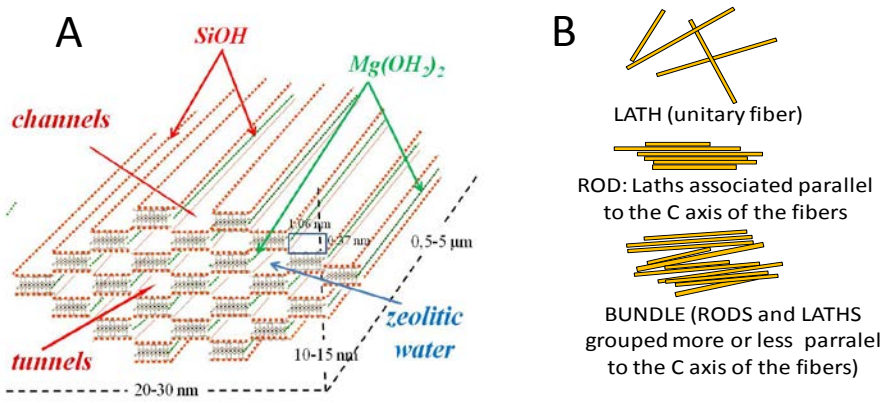

Figure 1. A) Schematic presentation of individualized sepiolite fibbers (LATH). B) Types of arrangement of sepiolite fibbers. “C axis” is the axis on the length of the fibber

Due to these properties, the control of the sepiolite organization inside the polymer matrix could be of great interest to provide nanometric control of materials and devices. However, the performances of nano-composites are related to the ability to well disperse the fillers and to control their distribution and organization insight the organic matrix. The introduction of natural nanofillers in the epoxy matrix will allow realizing fully non-toxic and sustainable organic-inorganic hybrid nanomaterials. Furthermore, our study is oriented to the control of the size, organization, dispersion and distribution of sepiolite into the bio-based thermoset. Firstly, the sepiolite’s dispersion into ELO homopolymer was studied. The efficiency of high shear mixing (UT) and high energy mixing (US) were used and compared in order to identify the process allowing to isolate the sepiolite fibbers in bundles and rods. Secondly, the same investigation was conducted on ELO/AcDiC copolymerization system. The addition of an initiator of copolymerization reaction was employed in this case. The obtained microstructures were characterized by transmission electronic microscopy (TEM) for all synthesized nanocomposites. The thermomechanical properties of ELO/AcDiC/sepiolite nanocomposites were also evaluated by dynamic mechanical (DMA) and thermogravimetric analysis (TGA).

2. Materials and method

2.1. Materials

A commercially available bio-based epoxy monomer was obtained from Akcros Chemicals Ltd (current Valtris). It is an epoxidized linseed oil (ELO) (figure 2) that is a viscous-liquid (~ 1.2 $Pa.s^{-1}$ at 25 °C). ELO has a molecular weight of about 980 $g.mol^{-1}$ and contains about 5.5 epoxy groups per triglyceride, on average. 2-methylimidazole (2-MI), with 99 % purity and supplied from Sigma-Aldrich, was used as crosslinking initiator. Sepiolite S9 was provided by TOLSA. A laboratory made bio-based crosslinking agent (the propylene glycol dimaleate), named AcDiC (figure 2) was used to cure ELO[17] [18].

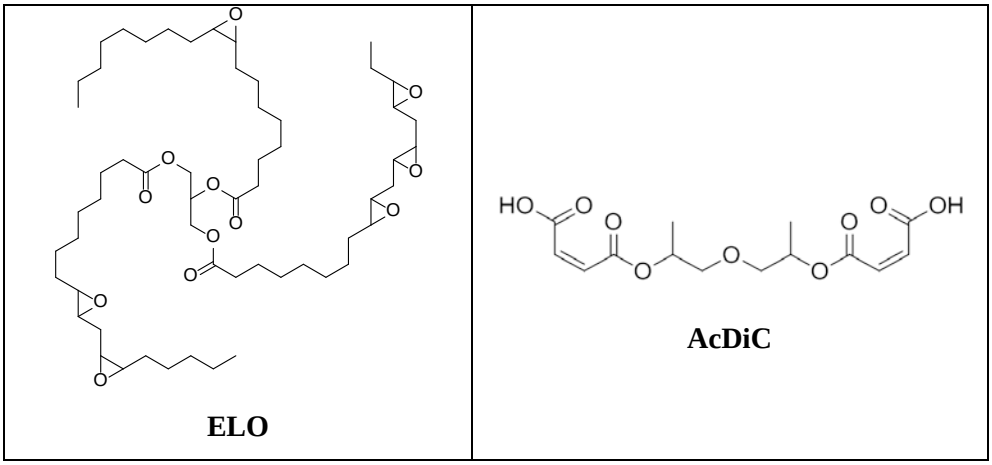

Figure 2: Chemical structure of epoxy monomer (ELO) and hardener (AcDiC)

2.2. Sepiolite and nanocomposites preparation

2.2.1 Sepiolite pre-treatment

To optimize its dispersion insight the organic matrix, the sepiolite was pre-treated in order to better separate the fibbers, prior to its mixing with the ELO based systems. For this, the sepiolite has been firstly dispersed in water by sonication. A suspension of 2 % of sepiolite powder was mechanically treated by sonication in water with the help of a high power ultra-sonication (US) waves (BIOBLOCK 20 kHz – 750 W, microprobe 3 mm for 10 min). The obtained suspension was then dried at 110 °C and the resulting clay was grinded to form the

pre-sonicated sepiolite powder. In this work, all nanocomposites were synthesized from this pre-sonicated sepiolite (PS).

2.2.2 Protocol of the sepiolite dispersion in neat ELO monomer

The PS sepiolite was dispersed at room temperature insight the neat ELO monomer by ultrasonication (US) (BIOBLOCK 20 kHz – 750 W) or by high shear mixing with ultraturrax (UT) (Ultraturrax® T-25). Dispersion conditions of the US and the UT pathways are shown in figure 3. The comparison between the two pathways is interesting as the energy provided for each technique is different (higher energy provided by US pathway). The idea is to highlight the effect of this energy of mixing on the quality of the sepiolite dispersion and on the final composites morphologies.

The resulting ELO/sepiolite suspensions provided great stability (any dephasing or sedimentation) over the time (several weeks) for the both dispersion pathways.

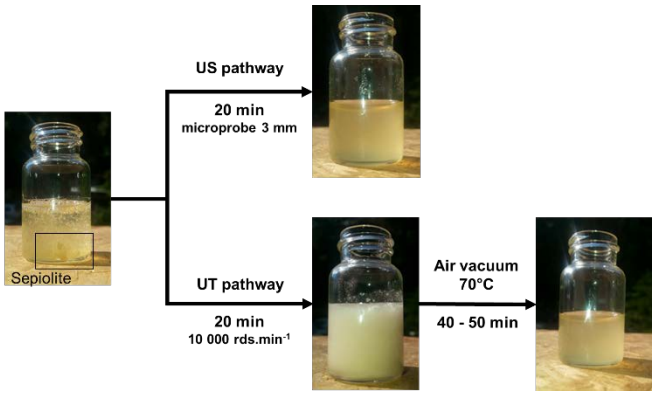

Figure 3. Photos showing the dispersion of sepiolite (1 % w/w) into ELO at room temperature by ultra-sonication (US) or by ultra-turrax (UT)

2.2.3 Sepiolite/neat ELO homopolymer (primary nanocomposites)

As ELO provides homopolymerization [18], the sepiolite was firstly dispersed into the ELO in order to compare their compatibility. 1 % weight of PS sepiolite was dispersed insight the neat ELO monomer by US and UT pathway following the previously detailed protocol

(Figure 3). Once the dispersion achieved, the homopolymerization was carried out at 180 °C for 24 hours. The resulting materials are defined as primary nanocomposites.

2.2.4 Nanocomposites synthesized with sepiolite and all reactant compounds of the epoxy resin (ELO, AcDiC and 2-MI initiator) (secondary nanocomposites)

Freshly ELO/sepiolite suspensions dispersed by US or UT pathway (Figure 3) were mixed during few minutes by magnetic stirring at 60 °C with AcDiC hardener and 1 % weight of 2-MI initiator. The mixtures have been formulated with a R ratio of 0.8 (R = AcDiC carboxylic acid groups/ELO epoxy groups). It is to note that a functional R ratio of 0.8 between ELO and AcDiC corresponds to a mass ratio of 50/50 w/w. The formulations were then cured 30 minutes at 150 °C and the post-curing was done during 30 minutes at 180 °C. The resulting materials are defined as secondary nanocomposites.

All sepiolite percentages of primary and secondary synthesized nanocomposites discussed below are expressed in mass ratio (wt. %).

2.3. Experimental techniques

Scanning electron microscopy (SEM) was used to study the contribution of sepiolite's pre-treatment. The SEM examinations were performed with a JEOL (6700F). Before the observation, samples were gold sputtered.

The morphologies of sepiolite nanocomposites were investigated by Transmission Electron Microscopy (TEM) at the Microscopy Center of University Nice Sophia Antipolis using a JEOL 1400. The samples were previously cut with the help of an ultra-microtome RMC power tome (~ 100 nm thick).

The dynamic mechanical properties were determined on a Triton Technology DMA equipped with STAR© software for curve analysis. The DMA was operated in traction mode with

sample dimensions of 15mm (length) x 4.5mm (width) x 1.5mm (thickness). Elastic modulus values (E') and damping factors (*tan δ*) were collected at 2 °C.min^{-1} heating rate from -20 to 80 °C and 1 Hz frequency. The glass transition temperature (T_α) was assigned at the maximum of damping factor (*tan δ* = E'/E'').

Thermogravimetric measurements (TGA) were conducted on a TGA 851e from Mettler-Toledo. The microbalance has a precision of ±0.1 µg. In order to evaluate the thermal stability of final materials, samples of about 15 mg were placed into 70 µL alumina pans. The measurements were performed at 10 °C.min^{-1} heating rate from 50 to 700 °C under 50 mL.min^{-1} air flow.

3. Results and interpretations

3.1 The advantage of pre-sonication process

As the ultra-sonication is not very effective in the ELO because of its viscosity (~ 1.2 Pa.s^{-1} at 25 °C), the sepiolite was firstly sonicated in water to transform the maximum of massive aggregates in small bundles ~~and rods~~ (Figure 4). The ultra-sonication is very effective in water because of its low viscosity and high volume pressure. Figure 4A and Figure 4B show SEM micrographs of dried sepiolite observed before and after the sonication process. The large aggregates were broken to favour the formation of small bundles, ~~rods and laths~~ (Figure 4B). This pre-treatment is therefore necessary to efficiently disperse the sepiolite in the epoxy matrix. The PS sepiolite fibbers behaviour was determined into neat ELO (primary nanocomposites) or within the all resin compounds (secondary nanocomposites).

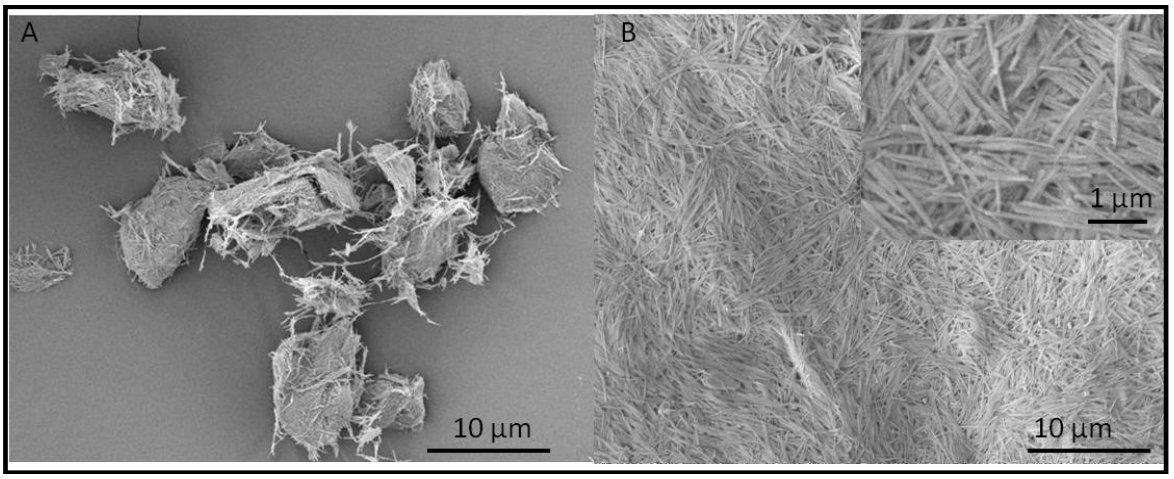

Figure 4: SEM micrographs of A) fibber massive aggregates of the virgin sepiolite. B) dispersed fibbers rods of sepiolite after the pre-sonication process of the sepiolite (PS sepiolite)

3.2. Primary nanocomposites synthesized from ELO/PS sepiolite

Samples with 1 % of PS sepiolite in neat ELO were homopolymerized (without AcDiC and 2-MI) to study their direct interaction and compatibility. Figure 5 displays the TEM micrographs of 1 % samples elaborated with UT pathway (Figure 5A) and US pathway (Figure 5B). Bundles ~~together with some rods~~ with an average distribution are observed for UT mixed samples (Figure 5A). A better dispersion ~~of rods and the presence of some bundles are~~ is observed for sonicated samples (Figure 5B). As a result, the dispersion of PS sepiolite by US or UT pathway in ELO homopolymer allows obtaining a good dispersion and distributions of sepiolite fibbers ~~rods~~ without its surface modification or the help of additives. ELO and fibbers seem enough compatible to allow fibbers isolation.

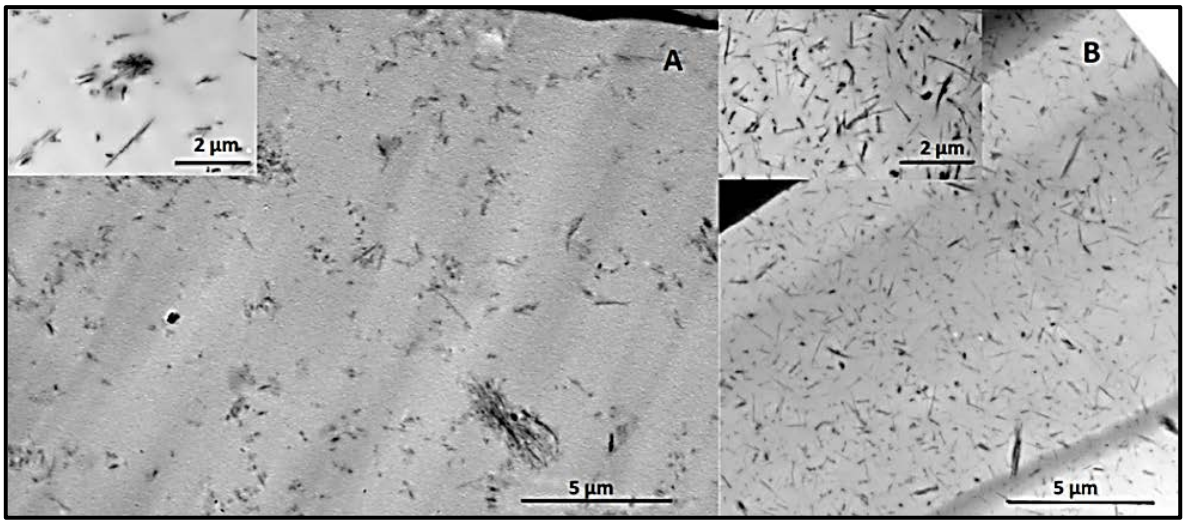

Figure 5. TEM nanocomposites micrographs of primary nanocomposites (ELO with 1 % of PS sepiolite) from A) UT and B) US pathway

3.3. Secondary nanocomposites

3.3.1. Secondary nanocomposites obtained by US pathway

The Figure 6 shows the visual appearance of secondary nanocomposites (i.e. when the sepiolite is cured with all reactant compounds of the epoxy resin). This figure shows an increase of opacity with the increase of the sepiolite percentage.

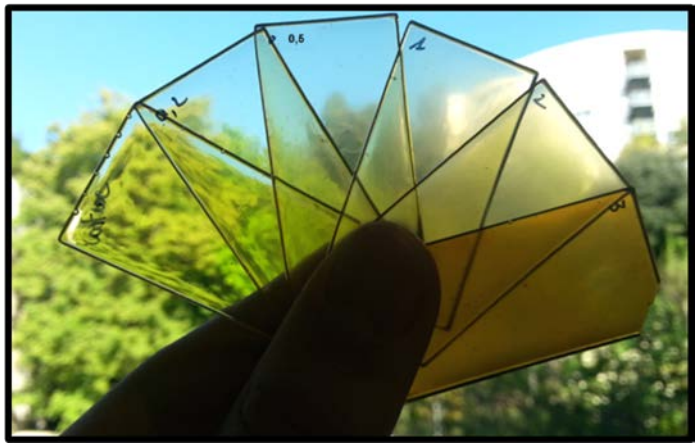

Figure 6. Visual aspect of secondary nanocomposites synthesized by US pathway. From left to right: reference thermoset (0 % of sepiolite), then nanocomposites with 0.2, 0.5, 1, 2 and 3 % of sepiolite

Figure 7 shows TEM micrographs of the secondary nanocomposite synthesized with 1 % of PS sepiolite from US pathway. We can observe in this figure several large circles (discoid) of micrometric size, constituted of sepiolite fibbers distributed on a border with organic matrix

inside and outside. The internal and external part of the sphere is constituted of epoxy resin. The micrographs show the presence of thin polymer thickness between ~~rods~~ fibbers and large polymer regions between ~~rod~~ fibbers groups that compose the sphere border contour (Figure 7D). Numerous regions full of polymer and empty of fibbers suggest that the ELO and AcDiC molecules are free to mix before polymerizing (Figure 7D). We can evoke that in ELO the sepiolite rods were well dispersed and distributed (Figure 5B). Then, the presence of the AcDiC and the 2-MI implies a drastic reorganization of sepiolite. This association has been formed during the ELO/AcDiC mixing step, the ~~rods~~ fibbers organizing in spheroid structures. Figure 7C and Figure 7D show the aggregation of these spheres toward larger spheroid structures. The analysis of a secondary nanocomposite with 0.5 % of PS sepiolite dispersed via US pathway has conducted to the same observation with the formation of sepiolite empty spheres, which are smaller in this case.

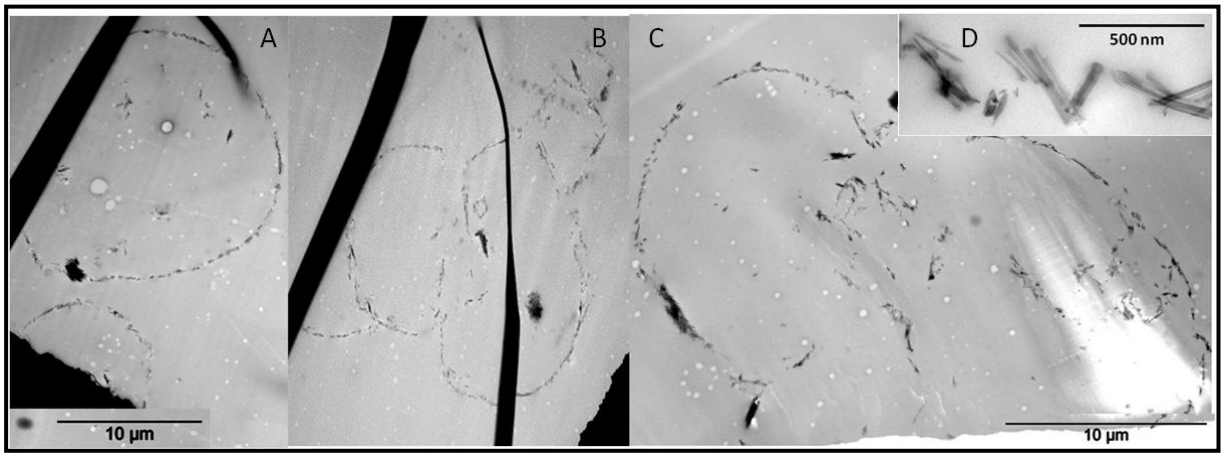

Figure 7: TEM micrographs of secondary nanocomposite synthesized from US pathway with 1 % of PS sepiolite: A) isolated spheroids, B) spheres in contact, C) sphere aggregates, D) sepiolite organization in the membrane at high magnification

By the same protocol a 2 % PS sepiolite secondary nanocomposite was produced. Figure 8 shows TEM micrographs of the resulting material. Numerous isolated ~~rods and~~ bundles that have a tendency to associate are observed. Spheroids are minority structures (Figure 8B). The previous fibbers organization seems to be impeded. This can be related to the specificity of fibbers dispersion: the fibbers suspension behaviour is related to regime of volume fraction. The sepiolite fibbers present a special behaviour in diluted (free to move), semi diluted (rotation in a single plane) and concentrated

(strong constraint) suspensions. In this nanocomposite, the constraints between ~~rods~~ fibbers can block theirs ~~mobility of the fibbers~~ and consequently theirs reorganization. Then, the formation of nanocomposites with homogeneously dispersed and distributed fibbers is favoured. These constraints imply an increase of viscosity that stabilizes the sepiolite in suspension during crosslinking.

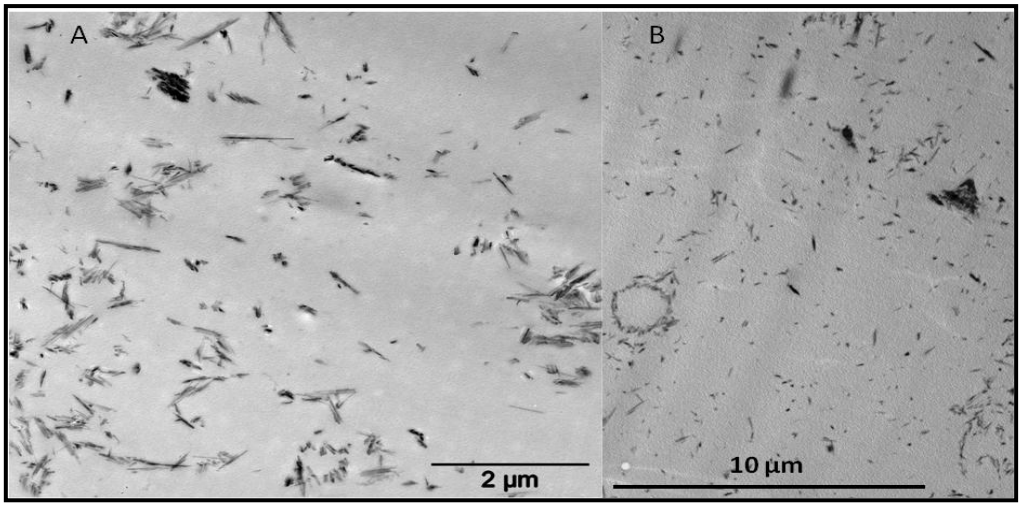

Figure 8: TEM micrograph of secondary nanocomposite synthesized from US pathway with 2 % of PS sepiolite

We propose three hypotheses for the mechanism of formation of these circles constituted by a phase rich in sepiolite and poor in resin. *i)* Firstly, the very thin polymer membranes rich in sepiolite are developed during polymerization; these membranes are forming spheres to minimize surface energy. *ii)* Another mechanism could be the association of fibbers at the interfaces of two different phases created during the addition step of AcDiC and 2-MI in the ELO/sepiolite suspension. The location of sepiolite at interface is known to be favoured if phase separation occurs. In literature, fibers as sepiolite or carbon nanotubes are sometimes partially or totally located at the interface of two immiscible components (REF), usually this organization is stabilized by this interface and the presence of the two phases is detected which is not the case here. The clay/resin interactions could have blocked the structure while ELO and AcDiC slowly become homogeneous and polymerize. The structure is related to memory form of sepiolite organization *iii)* The third hypothesis is the formation of clusters during the formation of 3D network assembly during crosslinking, specific for the epoxy

thermosets evolution. More dense regions characteristics of bridging between polymers chains growth in the 3D directions are generating triglyceride clusters. The sepiolite fibbers are excluded from these reacting regions through the surface of clusters, designing the spheres observed in TEM micrographs.

All these mechanisms are observed ~~possible~~ only if the fibbers are free to move, that means for low sepiolite concentration. When the sepiolite concentration increases, the self-organization conditions are modified and the sepiolite dispersion looks like its organization in neat ELO. In order to clarify this mechanism, a rheological study of these systems is in progress.

3.3.2. Secondary nanocomposites obtained by UT pathway

Figure 9 shows a 1 % PS sepiolite secondary nanocomposite formulated by UT pathway. The large full circles of fibbers relate in 3D to sepiolite full spheroids. The spheres are constituted of bundles (rods quasi parallel arranged) dispersed into the sphere bulk. The sphere sizes vary from 2 µm up to 20-30 µm. Compared to the primary nanocomposites resulting from UT dispersion (Figure 5A), there is a drastic change in the fibber distribution. We can observe domains without any fibbers out of the spheroids. However, this sepiolite dispersion into the spheres is similar to the UT pathway primary nanocomposite with a low increase of the bundle density (Figure 9 versus Figure 5A). The analysis of the same system with 0.5 or 2 % of PS sepiolite leads to the same observation with the formation of sepiolite full spheres (table 1) which are larger with the increasing percentage. From 2 % in sepiolite some bundles are present out of the spheroids.

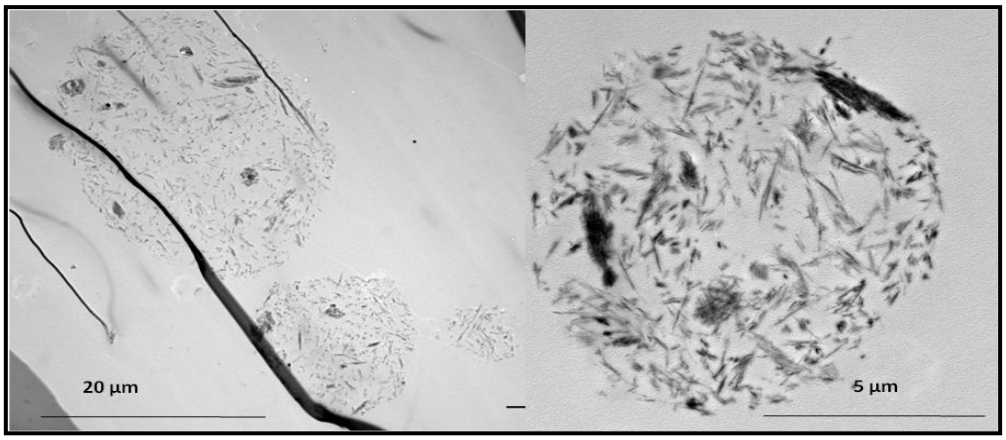

Figure 9: TEM micrographs of secondary nanocomposite synthesized from UT pathway with 1 % of PS sepiolite

Table 1. Sepiolite organization in nanocomposites made with secondary nanocomposites. Influence of dispersion technique and PS sepiolite percentage

		Sepiolite organization		
Dispersion pathway	**Mass of sepiolite (%)**	**Well distributed isolated fibbers** 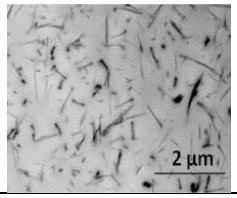	**Full spheroid** 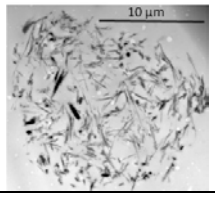	**Empty spheroid** 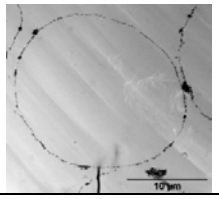
Ultra-turrax (UT)	0.5		X	
	1		X	
	2		X	
Ultrasonication (US)	0.5			X
	1			X
	2	X		

The sepiolite reorganization depends not only on the interactions ELO/sepiolite, AcDiC/sepiolite, and 2-MI/sepiolite but also on the energy afforded for mixing. Magnetic stirring associated with the heating up to 60 °C is the normal process used to obtain homogeneous ELO/AcDiC/2-MI suspensions [18]. We suppose that in this case, the energy is sufficient to homogenize ELO and AcDiC but not necessary to disperse the large bundles of sepiolite in the whole matrix. The bundles obtained by UT dispersion tend to associate in ELO or in AcDiC during the phase separation observed at the beginning of the ELO/AcDiC

mix. This association is restricted because of a certain concentration of fibbers, the acicular form of the bundles blocking the reorganization.

To conclude, the sepiolite organization is affected and the distribution is completely changed. The stability of the fibber organization during the polymerization process supposes strong interactions between sepiolite and ELO. Thus, it is not being excluded that the sepiolite influences the polymerization state in the spheres.

The observed dispersions are very different that has been reported in the literature [26] [27] [29] [50] [51]. Furthermore, the difference in the sepiolite organization in the nanocomposites obtained with secondary nanocomposites is directly related to the sepiolite dispersion technique applied in ELO. The large bundles present in the UT primary nanocomposites (Figure 5A) lead to filled sepiolite spheres (Figure 9) while the small bundles ~~rods~~ present in the US primary nanocomposites (Figure 5B) lead to empty spheres (Figure 8). When the ELO/sepiolite suspension and the AcDiC are mixed and homogenized, the large bundles conserve a similar organization while the smaller bundles ~~rods~~ are kept away from the ELO and AcDiC mixtures and self-associate into a spheroid configuration.

What draws attention in these results is the unusual behaviour of sepiolite in ELO based system. Self-organizations into spheres (liposomes, vesicles, emulsions, micelles) are strongly related to the HLB (Hydrophilic-Lipophilic Balance) ratio and the surfactant geometry. The self-organization of solid particles is described as depending on the concentration, the temperature, the formulation but also the size and wettability of these particles [52].

Wettability of sepiolite is related to hydrophilic $Mg(OH_2)_2$ groups in external channels and silanol groups on the side of hydrophobic talc-like ribbons (Figure 1A) [53]. This provides a hydrophilic/hydrophobic character of the sepiolite surface that is in contact with ELO. Thus, modifications on the surface will produce a change of organic matrix versus sepiolite interactions and their interfacial adsorption.

3.4. Thermomechanical properties of secondary nanocomposites

The thermal stability of synthesized nanocomposites was evaluated by TGA. Thermograms of nanocomposites containing PS sepiolite dispersed from US and UT pathways are displayed in Figure 10. The thermogram of an unfilled polymer was also included for comparison. The $T_{10\%}$ values (see insert of Figure 10A and Figure 10B) of nanocomposites are slightly lower than the $T_{10\%}$ unfilled polymer. Thus, the addition up to 2 % of sepiolite (with the different resulting dispersions) has no significant effect on the thermal stability of the epoxy nanocomposites with a thermal stability more than 300 °C. This tendency is in agreement with other epoxy/sepiolite systems [30] [31] [50] [51]. The bigger $T_{10\%}$ difference is observed for the nanocomposite with 2 % PS sepiolite dispersed by UT. This would be due to a greater distribution of the sepiolite fibbers caused by the formation of larger spheres.

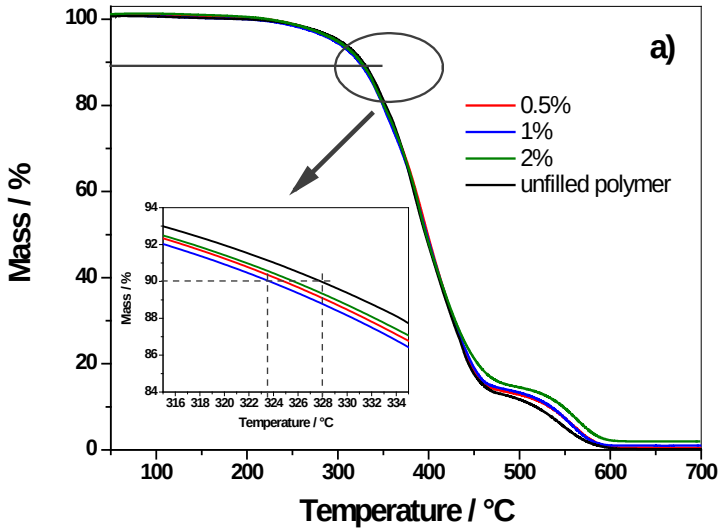

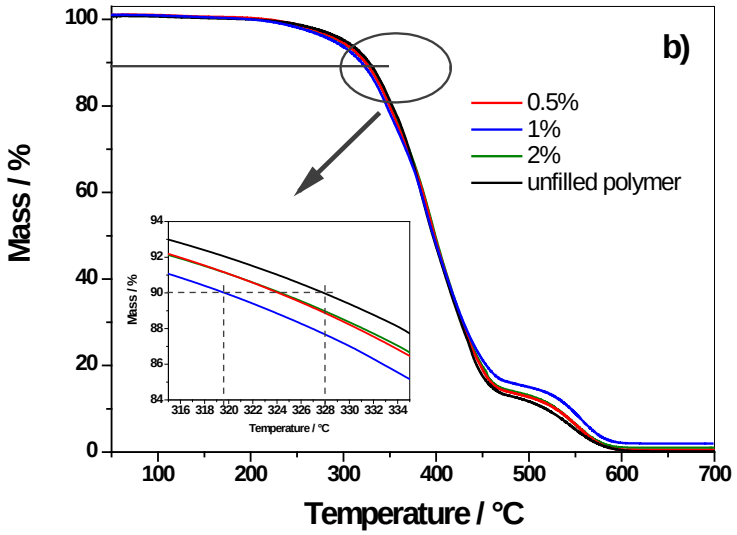

Figure 10: Thermal stability of different nanocomposites synthesized with 0.5, 1 and 2 % of PS sepiolite and dispersed by a) US or b) UT route. Insert: $T_{10\%}$ zoom. An unfilled polymer is added for comparison.

The Figure 11 exhibits the elastic moduli (in solid lines) and damping factors (*tan δ*) (in dotted lines) of nanocomposites dispersed by US and UT pathways. The DMA of an unfilled polymer was also included for comparison. The addition of sepiolite induces some modifications in the mechanical behaviour as the increasing of the elastic modulus from 30 to 40 % in the vitreous states and from 25 to 45 % in the rubbery state following the two dispersion pathways. This result is in agreement with other epoxy/sepiolite systems [29] [31] [51] due to the rigidity of sepiolite fibbers. E' moduli also show a drop of about two decades around the room temperature for all the systems. This decrease is attributed to the cooperative α-relaxation process of polymer chains, commonly associated with the glass transition (T_α). The resulting *tan δ* peak's height of this relaxation can also be directly correlated to the stiffness of systems. These curves show lower peak heights of all nanocomposites compared to the unfilled polymer and confirm the reinforcement of the organic matrix in presence of sepiolite.

The glass transition (T_α) of materials was assigned at the maximum of *tan δ* curves. As observed in Figure 11, the T_α of the unfilled polymer (T_α = 41 °C) is slightly higher than that

of all nanocomposites (30 °C < T_α > 34 °C). The sepiolite is known to modify the T_α value of the materials [29] [30] [31]. This decrease in T_α values could be explained because of the surface of the sepiolite is not functionalized [51] or linked to the organic network by covalent bonds. Thus, the intercalated fibbers between polymer chains may decrease the crosslink density of the organic matrix [54] by the decreasing of chemical reactions (esterifications, etherification or homopolymerization [55]) that are commonly observed in epoxy resin systems during the polymerization. The decrease of the degree of crosslinking could also be enhanced by the forms of sepiolite (in sphere full or empty), as already mentioned.

To sum up, the addition of sepiolite, and the different observed dispersion of its fillers, has a little effect on the thermal stability and the T_α values of the materials. However, this natural clay allows to significantly increase the modulus in both vitreous and rubbery state.

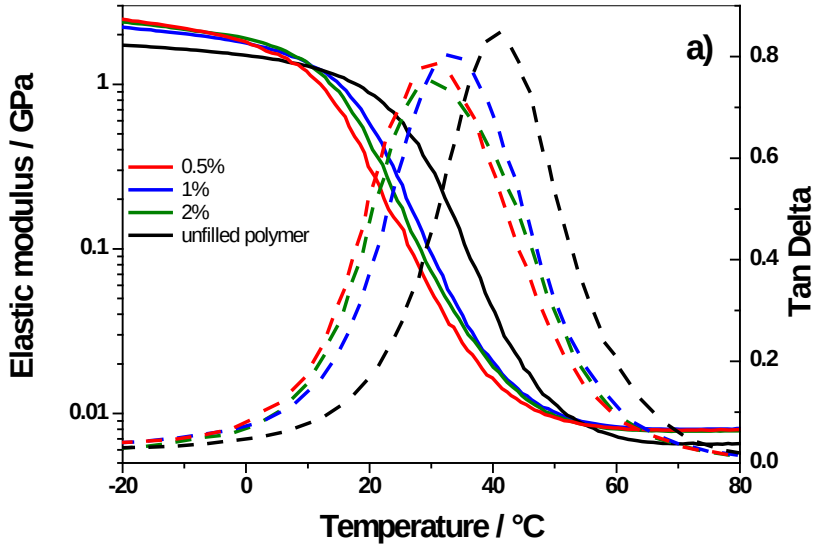

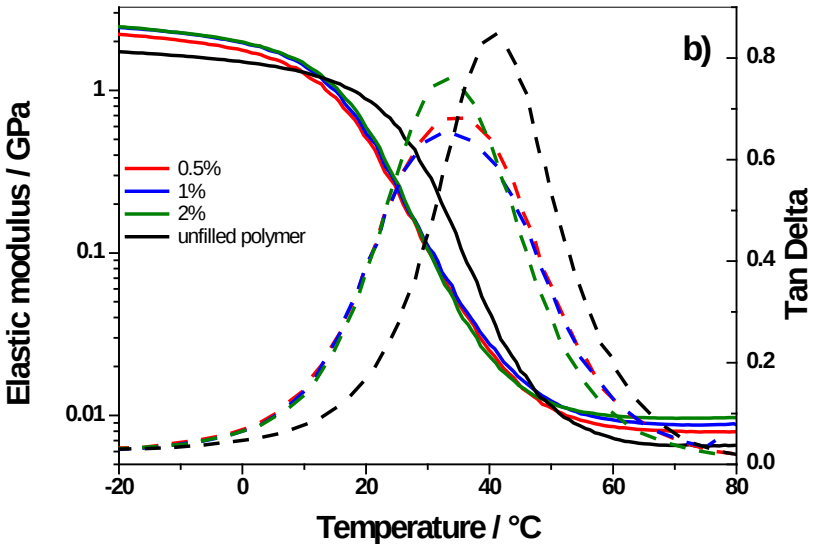

Figure 11: Mechanical behaviour as a function of temperature of secondary nanocomposites synthesized from 0.5, 1 and 2 % of PS sepiolite and dispersed by a) US and b) UT route. An unfilled polymer is added for comparison.

4. Conclusions

In this work, we have shown that it is possible to control and optimize the dispersion state of inorganic nanofiller into bio-based epoxy matrix without need to improve their interactions by adding chemical modification of the filler. Under certain conditions still to be deepened, the sepiolite behaves as a surfactant during the synthesis of the polymer based on ELO. Depending on the dispersion techniques, we obtained in a reproducible way *i)* large full or *ii)* empty spheroids of sepiolite fibbers, well dispersed and distributed.

The highlighted uncommon dispersions have no significant impact on the thermomechanical properties and thermal stabilities of final nanocomposites. However, the addition of sepiolite provokes an increasing of E' modulus up to 40 – 45 % in both vitreous and rubbery state following the two dispersion pathways.

To conclude, the hydrophilic/hydrophobic character of sepiolite, its very important specific surface area and its fibbers dimensions greatly influences their mixing, dispersing and distributing behaviour. Thus, numerous organizations are possible, ~~that can imply a very~~ works are in progress to better specify this interesting optical and rheological behaviour.

References

[1] H. Lee, K. Neville, Handbook of Epoxy Resins, Mc Graw-Hill, New York, 1982.

[2] J.-P. Pascault, R. J. J. Williams, Epoxy Polymers: New Materials and Innovations, Wiley-VCH, Weinheim, 2010.

[3] Y.-W. Mai, Z.-Z. Yu, Polymer nanocomposites, Wiley-VCH, Weinheim, 2006.

[4] V. Mittal, Optimization of polymer nanocomposite properties, Wiley-VCH, Weinheim, 2009.

[5] P. Gomez-Romero, C. Sanchez, Hybrid materials. Functional properties. From Maya Blue to 21st century materials, New J. Chem, 29 (2005) 57-58.

[6] C. Sanchez, B. Julian, P. Belleville, M. Popall, Applications of hybrid organic–inorganic nanocomposites, J. Mater. Chem. 15 (2005) 3559-3592.

[7] C. Laberty-Robert, K. Valle, F. Pereira, Design and properties of functional hybrid organic–inorganic membranes for fuel cells, Chem. Soc. Rev. 40 (2011) 961-1005.

[8] C. Sanchez, P. Belleville, M. Popall, L. Nicole, Applications of advanced hybrid organic-inorganic nanomaterials: from laboratory to market, Chem. Soc. Rev. 40 (2011) 696-753.

[9] F. Mammeri, E. L. Bourhis, L. Rozesa, C.Sanchez, Mechanical properties of hybrid organic–inorganic materials, J. Mater. Chem. 15 (2005) 3787–3811.

[10] L. Nicole, C. Laberty-Robert, L. Rozesab, C. Sanchez, Hybrid materials science: a promised land for the integrative design of multifunctional materials, Nanoscale 6 (2014) 6267–6292.

[11] M. A. R. Meier, J. O. Metzger, U. S. Schubert, Plant oil renewable resources as green alternatives in polymer science, Chem. Soc. Rev. 36 (2007) 1788-1802.

[12] R. Auvergne, S. Caillol, G. David, B. Boutevin ,J.-P. Pascault, Biobased thermosetting epoxy: present and future., Chem. rev. vol. 114 (2014) 1082-115.

[13] J. M. Pin, N. Sbirrazzuoli, A. Mija, From epoxidized linseed oil to bioresin: an overall approach of epoxy/anhydride cross-linking. ChemSusChem 8 (2015) 1232-1243.

[14] Y. Xia, R. C. Larock, Vegetable oil-based polymeric materials: synthesis, properties, and applications, Green Chem. 12 (2010) 1893-1909.

[15] G. L. Téllez, S. Hernández-López, Characterization of linseed oil epoxidized at different percentages, Superf. vacío 22 (2009) 5-10.

[16] M. R. g. Klaas, S. Warwel., Complete and partial epoxidation of plant oils by lipase-catalyzed perhydrolysis., Industrial Crops and Products, 9 (1999) 125–132.

[17] D. T. Carter, N. Stansfield, R. J. Mantle, C. M. France, P. A. Smith, An investigation of epoxidised linseed oil as an alternative to PVC in flooring applications, Ind. Crop. Prod. 28 (2008) 309-319.

[18] G. Falco, PhD Thesis : Huiles végétales époxydées et alcool furfurylique : deux types de monomères pour l'élaboration de thermodurcissables et de composites biosourcés, Université Nice Sophia Antipolis, 2016.

[19] B. Chena, J. R. G. Evans, Impact strength of polymer-clay nanocomposites, Soft Matter 5 (2009) 3572–3584.

[20] M. Darder, P. Aranda, E. Ruiz-Hitzky, Bionanocomposites: A new concept of ecological, bioinspired, and funcional hybrid materials, Adv. Mater. 19 (2007) 1309-1319.

[21] Y. Shchipunov, Bionanocomposites: Green sustainable materials for the near future, Pure Appl. Chem. 84 (2012) 2579–2607.

[22] M. M. Reddy, S. Vivekanandhan, M. Misra, S. K. Bhatia, A. K. Mohanty, Biobased plastics and bionanocomposites: Current status and future opportunities, Prog. in Polym. Sci. 38 (2013) 1653–1689.

[23] E. Ruiz-Hitzky, M. Darder, F. M. Fernandes, B. Wicklein, A. C. Alcântara, P. Aranda, Fibrous clays based bionanocomposites, Prog. Polym. Sci. 38 (2013)1392– 1414.

[24] E. Ruiz-Hitzky, P. Aranda, M. Darder, G. Rytwo, Hybrid materials based on clays for environmental and biomedical Applications, J. Mater. Chem. 20 (2010) 9306–9321.

[25] E. Ruiz-Hitzky, K. Ariga, Y. Lvov, Bio-inorganic Hybrid Nanomaterial - strategies, syntheses, characterisation and applications, Wiley-VCH, Weinheim, 2008.

[26] N. Volle, L. Challier, A. Burr, F. Giulieri, S. Pagnotta, A. Chaze, Maya Blue as natural coloring fillers in a multi-scale polymer-clay nanocomposite, Compos. Sci. Tech. 71, (2011) 1685–1691.

[27] N. Volle, F. Giulieri, A. Burr, S. Pagnotta, A. Chaze, Controlled interactions between silanol groups at the surface of sepiolite and an acrylate matrix: Consequences on the thermal and mechanical properties, Mat. Chem. Phys. 134 (2012) 417– 42.

[28] E. Duquesne, S. Moins, M. Alexandre, P. Dubois, How can Nanohybrids Enhance Polyester/Sepiolite Nanocomposite Properties?, Macromol. Chem. Phys. 208 (2007)

2542–2550.

[29] E. Franchini, J. Galy, J.F.Gérard, Sepiolite-based epoxy nanocomposites: Relation between processing, rheology, and morphology, J. Colloid. Interf. Sci. 329 (2008) 38-47.

[30] A. Zotti, A. Borriello, A. Martone, V. Antonucci, M. Giordano, M. Zarrelli, Effect of sepiolite filler on mechanical behaviour of a bisphenol A-based epoxy system, Compos. Part. B 67 (2014) 400–409.

[31] P. Verge, T. Fouquet, C. Barrère, V. Toniazzo, D. Ruch, J. Bomfima, Organomodification of sepiolite clay using bio-sourced surfactants: Compatibilization and dispersion into epoxy thermosets for properties enhancement, Compos. Sci. Technol. 79 (2013) 126–132.

[32] F. Pignon, A. Magnin, J. Piau, G. Belina, P. Panine, Structure and orientation dynamics of sepiolite fibers–poly(ethylene oxide) aqueous suspensions under extensional and shear flow, probed by in situ SAXS, Rheol. Acta 48 (2009) 563–578.

[33] G. Tartaglione, D.Tabuani, G. Camino, M. Moisio, PP and PBT composites filled with sepiolite: Morphology and thermal behaviour, Compos. Sci. Technol. 68 (2008) 451-460.

[34] J. Ma, E. Bilotti, Preparation of polypropylene/sepiolite nanocomposites using supercritical CO2 assisted mixing, Eur. Polym. J. 43 (2007) 4931–4939.

[35] E. Bilotti, E. Duquesne, H. Deng, R. Zhang, F. Quero, S. N. Georgiades, H. R. Fischer, P. Dubois, T.Peijs, In situ polymerised polyamide 6/sepiolite nanocomposites: Effect of different interphases, Eur. Polym. J. 56 (2014) 131–139.

[36] E. Bilotti, R. Zhang, H. Deng, F. Quero, H. Fischer, T. Peijs, Sepiolite needle-like clay for PA6 nanocomposites: An alternative to layered silicates?, Compos. Sci. Technol. 69 (2009) 2587–2595.

[37] H. Chen, M. Zheng, H. Sun, Q. Jia, Characterization and properties of sepiolite/polyurethane nanocomposites, Mat. Sci. Eng. A 445–446 (2007) 725–730.

[38] K. Fukushima, D. Tabuani, G. Camino, Nanocomposites of PLA and PCL based on montmorillonite and sepiolite, Mat. Sci. Eng. C 29 (2009) 1433–1441.

[39] K. Fukushima, D. Tabuani, C. Abbate, M. Arena, L.Ferreri, Effect of sepiolite on the biodegradation of poly(lactic acid) and polycaprolactone, Polym. Degrad. Stab. 95 (2010) 12049-2056.

[40] M. Rautureau, C. Tchoubar, Structural analysis of sepiolite by selected area electron diffraction–relations with physico-chemical properties, Clays Clay Miner. 24 (1976) 43–49.

[41] C. Serna, J. Ahlrich, J.M. Serratosa, Folding in sepiolite crystals, Clays Clay Miner. 23 (1975) 452-457.

[42] G. Van Scoyoc, C. Serna, J. Ahlrichs, Am. Mineral. 64 (1979) 215-223.

[43] L. Bokobza, A. Burr, G. Garnaud, M. Perrin, S. Pagnotta, Fibre reinforcement of elastomers: nanocomposites based on sepiolite and poly(hydroxyethyl acrylate), Polym. Int., 53 (2004) 1060–1065.

[44] L. Bokobza, J. Chauvin, Reinforcement of natural rubber: use of in situ generated silicas and nanofibres of sepiolite, Polymer 46 (2005) 4144–4151.

[45] M. Sangerano, E. Pallaro, I. Roppolo, G. Rizza, UV-cured epoxy coating reinforced with sepiolite as inorganic filler, J. Mat. Sci. 44 (2009) 3165–3171.

[46] Z. Zhang, J. van Duijneveldt, Isotropic-nematic phase transition of nonaqueous suspensions of natural clay rods, J. Chem. Phys. 124 (2006) 154910.

[47] P. Woolston, J. van Duijneveldt, Isotropic–nematic phase transition in aqueous sepiolite suspensions, J. Colloid Inter. Sci. 437 (2015) 65-70.

[48] S. Ovarlez, F. Giulieri, F. Delamare, N. Sbirrazzuoli, A. Chaze, Indigo–sepiolite nanohybrids: Temperature-dependent synthesis of two complexes and comparison with indigo–palygorskite systems, Micropor. Mesopor. Mat. 142 (2011) 371–380.

[49] J. Raya, J. Hirschinger, S. Ovarlez, F. Giulieri, A. Chaze, F. Delamare, Insertion of indigo molecules in the sepiolite structure as evidenced by 1H–29Si heteronuclear correlation spectroscopy, Phys. Chem. Chem. Phys. 12 (2010) 14508-14514.

[50] A. Nohales, L. Solar, I. Porcar, C. I. Vallo, C. M. Gómez, Morphology, flexural, and thermal properties of sepiolite modified epoxy resins with different curing agents, Eur. Polym. J. 42 (2006) 3093-3101.

[51] A. Nohales, R. Muñoz-Espí, P. Félix, C. M. Gómez, Sepiolite-reinforced epoxy nanocomposites: Thermal, mechanical, and morphological behavior, J. App. Polym. Sci. 119 (2011) 539-547.

[52] B. Blinks, Particles as surfactants, similarities and differences, Curr. Opin. Int. 7 (2002) 21-41.

[53] B. Benli, H. Du, M. Celik, The anisotropic characteristics of natural fibrous sepiolite as revealed by contact angle, surface free energy, AFM and molecular dynamics simulation, Colloid. Surface A, 408 (2012) 22– 31.

[54] R. Ganfoud, L. Puchot, T. Fouquet, P. Verge, H-bonding supramolecular interactions driving the dispersion of kaolin into benzoxazine: A tool for the reinforcement of

polybenzoxazines thermal and thermo-mechanical properties, Compos. Sci. Technol. 110 (2015) 1-7.

[55] L. Shechter, J. Wynstra, Glycidyl Ether Reactions with Alcohols, Phenols, Carboxylic Acids, and Acid Anhydrides, Ind. Eng. Chem. 48 (1596) 86-93.